Theory of alloys. I. Embedded-cluster calculations of phonon spectra for a one-dimensional binary alloy

Charles W. Myles* and John D. Dow
Department of Physics and Materials Research Laboratory, University of Illinois at Urbana-Champaign, Urbana, Illinois 61801
(Received 8 January 1979)

By treating a small cluster embedded in an effective medium (described here by the coherent-potential approximation) we can reproduce the "exact" numerical frequency-distribution spectra of the vibrating-linear-chain alloy A_cB_{1-c} with mass disorder. The theory is especially applicable to concentrations $0.05 \lesssim c \lesssim 0.95$ throughout the alloy regime, where other theories are quantitatively unreliable. Unlike purely numerical calculations, the present method can be practically applied to real three-dimensional alloys. The theory is valid for all concentrations c and all mass ratios m_B/m_A; it satisfies the oscillator strength sum rule, and it reduces to the exactly soluble single-defect theory in the limits $c \to 0$ and $c \to 1$. Its greatest virtue is that it is computationally efficient, because it does not require large clusters.

I. INTRODUCTION

As a first step toward predicting the vibrational properties and luminescence sidebands[1] of III-V semiconducting nitrogen-doped ternary alloys such as $GaAs_{1-c}P_c$ and $Al_cGa_{1-c}As$, we consider here phonons in a mass-disordered random one-dimensional binary alloy A_cB_{1-c} of atoms coupled harmonically by nearest-neighbor forces and executing longitudinal vibrations. In this paper we present a conceptually simple, computationally-efficient scheme for calculating the vibrational spectra of this one-dimensional binary alloy model. The scheme, which we call the embedded-cluster method, is manifestly applicable to ternary alloys[2] and to three-dimensional systems as well.[3] We study this linear-chain model because it has been solved exactly (numerically) by Dean[4,5] and by Payton and Visscher[6] for chains of 8000 to 100 000 atoms; these numerical solutions therefore afford a convenient touchstone of comparison for the present less cumbersome but more approximate scheme for computing binary-alloy spectra. This one-dimensional model has proven difficult to simulate, and the prevailing opinion in the literature is that any method of approximation capable of rendering an accurate solution in one dimension should produce accurate predictions for three-dimensional solids as well.[7]

Analytic or perturbative statistical mechanical theories of one-dimensional binary alloy spectra are doomed to failure because a correct theory is necessarily nonanalytic in the concentraction c, the mass ratio m_A/m_B, and the frequency ω.[8] This nonanalyticity manifests itself physically by the sudden appearance of distinct local mode frequencies above the band when the concentration of light-mass defects is altered from zero to any infinitesimal value.

Direct numerical solutions of the equations of motion for 8000 to 100 000-atom linear binary alloys have been presented by Dean[4,5] and by Payton and Visscher.[6] These solutions, while providing the "exact" alloy spectra, are numerically cumbersome and would become impractical if applied to comparably-sized clusters in real three dimensional alloys.

What is needed is a hybrid theory which takes advantage of the assets of both the numerical and the statistical-analytical approaches; it must numerically treat finite clusters of atoms in order to properly determine the short-ranged correlations in atomic motions; and it must be partially an analytic effective-medium theory in order to circumvent the computational difficulties associated with the enormous clusters required by the purely numerical solutions. Some such methods, called multisite coherent potential approximations, have been proposed,[9-27] but to date have been numerically cumbersome because of their requirement that a spatially varying self-energy be determined self-consistently for a cluster of atoms. In this paper we present an alternative to these multisite coherent potential approximations, which though lacking self-consistency and therefore less rigorous theoretically, nevertheless can greatly reduce the computational labor at little loss of accuracy. The basic idea of the method is that a small cluster of atoms embedded in an effective medium should produce all the correct vibrational spectra of the alloy, provided the effective medium properly simulates the reflection and transmission coefficients for phonons leaving the cluster.

The remainder of the paper is organized as follows: Section II defines notation. The difficult binary alloy problem, namely $c = 0.5$, is discussed in Sec. III, where various theoretical schemes are reviewed. The requirements which must be satis-

fied by a successful theory are summarized in Sec. IV, and the present theory is presented in Sec. V. Section VI contains a comparison of the present theory with "exact" numerical calculations, and the results are discussed in Sec. VII. The Appendix contains a discussion of the average-T-matrix approximation and why it yields an unsatisfactory effective medium for an embedded cluster theory.

II. NOTATION: THE ONE-DIMENSIONAL VIBRATING LATTICE

A, Equations of motion for the alloy

The equations of motion for the linear chain are

$$m_n \ddot{u}_n = -\phi(-u_{n+1} - u_{n-1} + 2u_n) \ . \tag{1}$$

This equation can also be written in matrix form with $u_n(t) = \langle n|u\rangle e^{-i\omega t}$

$$-\underline{M}\omega^2|u\rangle = -\underline{\Phi}|u\rangle \ .$$

Here the matrices are $\langle n|\underline{M}|n'\rangle = m_n\delta_{n,n'}$ and

$$\langle n|\underline{\Phi}|n'\rangle = -\phi(\delta_{n',n+1} + \delta_{n',n-1} - 2\delta_{n',n}) \ .$$

The lattice constant is a and the longitudinal displacement of the atom at na is u_n. The nearest-neighbor forces are taken to be identical (with force constants ϕ), periodic boundary conditions are assumed ($u_{N+n} = u_n$), and the alloy disorder is limited to the masses m_n which may be either m_A or m_B in the alloy A_cB_{1-c}. Here we employ the convention that m_A is the lighter mass, and define the frequencies

$$\omega_A = (\phi/m_A)^{1/2} \ \text{and} \ \omega_B = (\phi/m_B)^{1/2} \ . \tag{2}$$

B. Solutions for an ordered monatomic lattice

If the two masses are equal, $m_B = m_A = m$, then the "alloy" is ordered, and the phonon dispersion relation becomes that for the perfect crystal[28]:

$$\omega^0(q) = \omega_m|\sin(qa/2)| \ , \tag{3}$$

where

$$\omega_m = 2(\phi/m)^{1/2}$$

and the wave vectors are $q = \nu\pi/Na$ with $\nu = 0, \pm1, \ldots$.

The Green's function is defined as

$$\underline{G}(\omega^2) = (\underline{M}\omega^2 - \underline{\Phi} + i0)^{-1} \tag{4}$$

where $i0$ is a positive imaginary infinitesimal. For the perfect monatomic linear chain, the in-band Green's function is,[28] for $\omega \leq \omega_m$,

$$\langle n+n'|\underline{G}^0(\omega^2)|n'\rangle = (\exp i|n|\chi)/2i\phi\sin\chi \ , \tag{5a}$$

where we have $\chi = 2\arcsin(\omega/\omega_m)$, with $0 < \chi < \pi$.

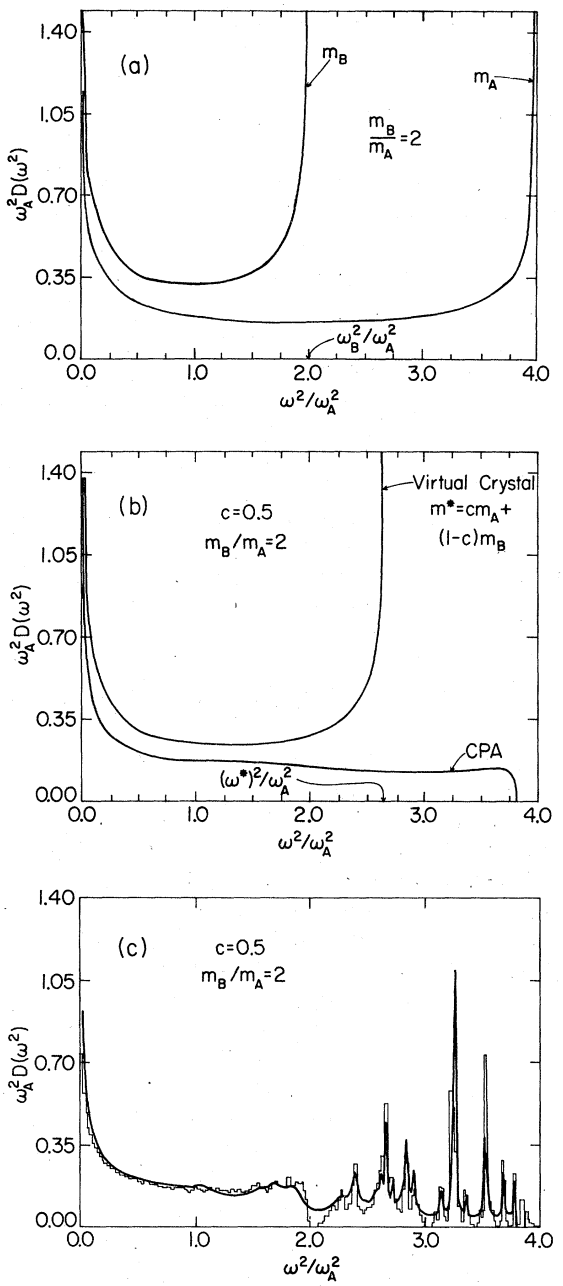

FIG. 1. Vibrational density of states (a) for the perfect linear chain, shown for two different masses with mass ratio $m_B/m_A = 2$; (b) for the one dimensional alloy A_cB_{1-c} in the virtual crystal approximation and in the coherent-potential approximation (CPA), shown for mass ratio $m_B/m_A = 2$ and for concentration $c = 0.5$; (c) for the alloy A_cB_{1-c}; the histogram is the exact vibrational density of states for the disordered linear chain A_cB_{1-c} obtained by Payton and Visscher (Ref. 6) for 100 000 atoms; the dark curve is the result obtained by the present embedded cluster method using a cluster of 10 atoms and a CPA effective medium. These are shown for mass ratio $m_B/m_A = 2$ and concentration $c = 0.5$.

When we have $\omega > \omega_m$, this function becomes

$$\langle n+n'|\underline{G}^0(\omega^2)|n'\rangle = (-1)^n[f-(f^2-1)^{1/2}]^{2|n|} \times [4\phi f(f^2-1)^{1/2}]^{-1} \quad (5b)$$

with $f=\omega/\omega_m$.

The density of states, or spectrum of squared frequencies, is

$$D(\omega^2) \equiv \frac{1}{N}\sum_q \delta(\omega^2-\omega^2(q)) = (-1/N\pi)\mathrm{Im}\,\mathrm{Tr}[\underline{M}\underline{G}(\omega^2)] \ , \quad (6)$$

where the sum on q runs over the first Brillouin zone. For the monatomic linear chain, this becomes[28]

$$D^0(\omega^2) = [\pi\omega(\omega_m^2-\omega^2)^{1/2}]^{-1}\theta(\omega_m^2-\omega^2) \ , \quad (7)$$

where θ is a unit step function. This result is displayed in Fig. 1(a) for two homogeneous chains whose masses differ by a factor of $2=\omega_A^2/\omega_B^2=m_B/m_A$.

III. THE DIFFICULT ALLOY PROBLEM: THE NECESSITY OF A NEW THEORY

One of the most difficult alloy problems is to obtain the vibrational density of states in the 50% concentration limit, $c=0.5$. As a measure of the success of a theory, we take its ability to reproduce the "exact" numerical density of states for $c=0.5$ and mass ratio $m_B/m_A=\omega_A^2/\omega_B^2=2$. The frequency spectrum for this case has been evaluated employing numerous analytical and numerical schemes[4-7] for the linear chain model, Eq. (1), thereby permitting comparison of the various methods.

A. Numerical solution

The "exact" solution of this problem has been obtained by Payton and Visscher[6] for a chain of 100 000 atoms using a numerical technique originally developed by Dean.[4,5] That solution is displayed in Fig. 1(c) and is inexact by an amount comparable to the structure of the boxes in the figure. For comparison we have also previewed the results of the present work in Fig. 1(c) to show that this new but simple scheme does accurately reproduce the "exact" result. The Dean method obtains the vibrational density of states by employing the negative eigenvalue theorem[4,5] and by using numerical simplifications which result from the tridiagonality of the dynamical matrix $M^{-1/2}\Phi M^{-1/2}$ for the one-dimensional nearest-neighbor-spring model. The tridiagonality does not carry over to *real* three-dimensional alloys, and so the Dean numerical method is, in practice, limited to such small clusters in three dimensions that its claim to exactness becomes doubtful.

B. Virtual crystal approximation

The vibrational density of states in the difficult alloy limit, $c=0.5$, $m_B/m_A=\omega_A^2/\omega_B^2=2$, is not simply related to the densities of states of the pure solids A and B. For example, the simplest estimate of the alloy density of states is given by the virtual crystal approximation: the density of states of a crystal with the average mass $m^*=cm_A+(1-c)m_B$.[7] The resulting frequency distribution [Fig. 1(b)] completely misrepresents the "exact" result because this approximation merely replaces the alloy by a perfect homogeneous crystal with a mass m^* on each site. Thus, the virtual crystal approximation omits the clustering and heterogeneous local fluctuations of alloy configurations which are responsible for characteristic peaks in the state density.

C. Statistical theories

1. The coherent potential approximation

In a more rigorous treatment of the alloy problem, one might seek the best quasinormal modes of a statistically averaged alloy. Therefore, instead of prescribing an average mass, as in the virtual crystal approximation, one specifies an average propagator or Green's function, in what is termed the coherent-potential approximation (CPA).[7,29-32] This average-medium Green's function $\underline{g}$ is fixed by the requirements (i) that the effective-medium quasiparticles scatter from each atomic site the minimum amount, that is, the single-site effective-medium transition matrix, when averaged over all possible alloy configurations, is zero (it is not practical to require that the multisite T matrix vanish); and (ii) that its self-energy $\underline{\Sigma}$ assume the mathematically simple form

$$\underline{\Sigma} = \sum_n |n\rangle\sigma(\omega)\langle n| \equiv \sum_n \underline{\sigma}_n(\omega) \ , \quad (8)$$

thereby giving a single frequency-dependent lifetime and level shift to all the quasinormal modes of the statistically averaged alloy. Requirement (ii) gives the simple result for the effective medium Green's function

$$\underline{g}(\omega^2) = \underline{G}^0(\omega^2 - m_B^{-1}\sigma(\omega)) \ , \quad (9)$$

where here, and throughout the rest of the paper, we take the reference lattice Green's function $\underline{G}^0(\omega^2)$ to be the perfect lattice Green's function for a lattice with all masses equal to m_B. (In the CPA, the choice of reference lattice is irrelevant, because the self-consistent CPA Green's function is invariant under a change of reference lattice.[7,29-32])

The exact Green's function for a specific alloy configuration satisfies the Dyson equation

$$\underline{G} = \underline{G}^0 + \underline{G}^0 \underline{V} \underline{G} , \tag{10}$$

where we have

$$\underline{V} = \underline{\Phi} - \underline{\Phi}_0 - (\underline{M} - \underline{M}_0)\omega^2 ; \tag{11}$$

for the mass-disorder model, $\underline{V}$ is diagonal and is nonzero only at A-atom sites:

$$\underline{V} = \sum_n \underline{v}_n \tag{12a}$$

with

$$\underline{v}_n = |n\rangle (m_B - m_n)\omega^2 \langle n| . \tag{12b}$$

The effective medium Green's function is defined as the configuration average of the alloy Green's function G,

$$\underline{g} = \langle\langle \underline{G} \rangle\rangle , \tag{13}$$

where the double brackets denote an ensemble average over all alloy configurations. In the CPA, the statistically averaged Green's function is assumed to satisfy

$$\underline{g} = \underline{G}^0 + \underline{G}^0 \underline{\Sigma} \underline{g} , \tag{14}$$

which results in the simple expression Eq. (9), where $\underline{\Sigma}$ is the (as yet unknown) self-energy. Eliminating $\underline{G}^0$ from Eqs. (10) and (14), one obtains

$$\underline{G} = \underline{g} + \underline{g}(\underline{V} - \underline{\Sigma})\underline{G} = \underline{g} + \underline{g} \sum_n (\underline{v}_n - \underline{\sigma}_n)\underline{G} . \tag{15}$$

The single-site effective-medium transition matrix is

$$\underline{\tau}_n \equiv (\underline{v}_n - \underline{\sigma}_n)[\underline{1} - \underline{g}(\underline{v}_n - \underline{\sigma}_n)]^{-1} . \tag{16}$$

In the CPA, the configuration average of τ_n must vanish, thus we have

$$\langle\langle \underline{\tau}_n \rangle\rangle = 0$$

$$= |n\rangle\langle n| \left(\frac{(1-c)(-\sigma)}{1 + \sigma\langle n|\underline{g}|n\rangle} + \frac{c[(m_B - m_A)\omega^2 - \sigma]}{1 - \langle n|\underline{g}|n\rangle[(m_B - m_A)\omega^2 - \sigma]} \right) , \tag{17a}$$

which results in the equation for $\sigma(\omega)$

$$\sigma(\omega) = \frac{c(m_B - m_A)\omega^2}{1 - \langle n|G^0(\omega^2 - m_B^{-1}\sigma(\omega))|n\rangle[(m_B - m_A)\omega^2 - \sigma(\omega)]} \tag{17b}$$

When combined with the known expression for $\underline{G}^0$, Eq. (17b) can be solved for the self-consistent self-energy $\sigma(\omega)$. For the one-dimensional linear-chain problem, using Eq. (5) for $\underline{G}^0$, and defining $\sigma(\omega) = m_B\omega^2\tilde{\sigma}(\omega)$, $X = \omega/2\omega_B$, and $\epsilon = 1 - m_A/m_B$, one finds the cubic equation for $\tilde{\sigma}(X)$,[30]

$$a_3\tilde{\sigma}^3 + a_2\tilde{\sigma}^2 + a_1\tilde{\sigma} + a_0 = 0 , \tag{18a}$$

where we have

$$a_3 = 2X^2[1 - \epsilon(1-c)] - 1 \tag{18b}$$

$$a_2 = X^2[\epsilon^2(1-c^2) - (4c\epsilon + 1)] + 2c\epsilon + 1 , \tag{18c}$$

$$a_1 = c\epsilon[2X^2(1 + c\epsilon) - (2 + c\epsilon)] , \tag{18d}$$

and

$$a_0 = c^2\epsilon^2(1 - X^2) . \tag{18e}$$

The CPA density of states takes the form[30]

$$D_{\mathrm{CPA}}(\omega^2) = -(1/N\pi)\,\mathrm{Im}[\mathrm{Tr}\langle\langle \underline{M}\underline{G} \rangle\rangle]$$

$$= -(1/\pi)\,\mathrm{Im}[m_B(1 - \tilde{\sigma})\langle n|\underline{G}^0(\omega^2(1 - \tilde{\sigma}))|n\rangle] . \tag{19}$$

This result is displayed in Fig. 1(b) for $m_B/m_A = 2$ and $c = 0.5$. Clearly, the CPA fails to reproduce the "exact" spectrum. (The CPA was not designed to reproduce the spectrum, but was constructed to properly mimic the long-wavelength properties of the lattice vibrations in the alloy.)

To order c or $1 - c$ in the concentration, the CPA reproduces the exact theoretical spectrum. But if pairs or larger clusters of defects contribute significantly to the density of states, the CPA breaks down. For example, for a mass ratio $m_B/m_A = \omega_A^2/\omega_B^2 > 1$, CPA predicts a local-mode frequency distribution which broadens from a δ function at $c \to 0$ into a nearly elliptical spectrum for any appreciable c. This is illustrated in Fig. 2 for the case $m_B/m_A = 100$. The exact result agrees with the CPA δ function at $c \to 0$, but gives rise to a single-defect spike plus a distribution of paired-defect sidebands as c increases from zero.

The failure of the CPA is due to the single site approximation, Eq. (8), for the self-energy. The CPA, similar to the virtual crystal approximation and all other single site theories, thus replaces the alloy by a perfect effective medium with the same (complex) mass on each site and totally neglects the local environment effects which are responsible for the peaked structures in the density of

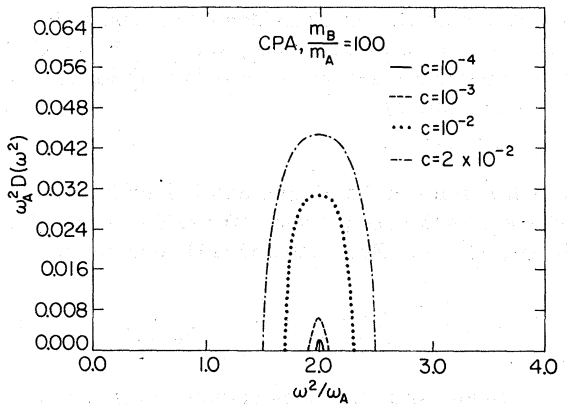

FIG. 2. Illustration of the change in the one dimensional coherent-potential approximation isolated local-mode δ function as the concentration is increased. Shown for $m_B/m_A = 100$ to bring out the local mode behavior most clearly.

states.[4-7] Although the CPA fails to give the correct density of states in the local mode region of of the alloy spectrum, we have found it very useful as an effective medium for use with our embedded cluster method, as discussed in Sec. V. This is no doubt because the CPA gives the best quasiparticles and does simulate the average long-wavelength properties of the random medium reasonably well.

2. *The average-t-matrix approximation*

The average-t-matrix approximation (ATA),[7] like the CPA, is a single-site approximation. It differs from the CPA in that the self-energy σ is not determined self-consistently, but is evaluated using Rayleigh-Schrödinger rather than Brillouin-Wigner perturbation theory. Thus $\langle n|\underline{g}|n\rangle$ in Eq. (17a) is replaced by $\langle n|\underline{G}^0|n\rangle$. The ATA is easier to execute than the CPA, but is of more limited theoretical validity. Like the CPA, it only reproduces the $c \to 0$ and $c \to 1$ limits correctly, and these limits, in the general case of a real alloy, are more easily evaluated using single-defect theory. Moreover, ATA does not meet our needs for an effective medium for use with our embedded cluster theory, as discussed in the Appendix, and so will be ignored throughout the remainder of this paper.

3. *Multiple-site coherent-potential approximation*

Several generalizations of the CPA have been proposed which account for the multisite scattering neglected in the ordinary CPA.[9-27] In principle, these generalizations should produce accurate alloy theories, provided a sufficient number of sites are included in the determination of a self-consistent self-energy $\underline{\Sigma}(\vec{k}, \omega)$. When applied to the current one dimensional phonon problem, the cluster CPA theories of Best and Lloyd,[18] Tsukada,[19] Takahashi and Shimizu,[20] and Wu[21,22] all achieve results which are in qualitative agreement with the exact numerical calculations of Dean[4,5] and Payton and Visscher,[6] and which are thus comparable with the results obtained by using the embedded cluster method outlined in Sec. V. However, because the multisite CPA methods determine a self-consistent wave-vector-dependent self-energy $\underline{\Sigma}(\vec{k}, \omega)$ for the cluster, the cluster equations must be iterated to a self-consistent solution, not just once (as in the ordinary CPA) but several times, once for each wave vector in the Brillouin-zone mesh. Moreover, the multisite CPA is plagued by nonanalyticities and occasionally-negative state densities[7]; therefore, the multisite CPA methods are judged to be computationally and aesthetically inferior to the present method.

IV. REQUIREMENTS ON A SUCCESSFUL APPROXIMATE THEORY OF ALLOYS

To be successful, a theory of phonons in alloy must be able to reproduce the "exact" numerical one-dimensional phonon densities of states (i) for the entire range of alloy concentrations c, (ii) for the entire range of persistence-amalgamation coupling constants $[(m_B - m_A)\omega^2/\phi]$, and (iii) with sufficient computational speed to be practical not only for one-dimensional systems but for real three dimensional alloys as well.

A. Concentration

The concentration scale can be roughly divided into three regimes (i) $c \lesssim 0.001$ or $c \gtrsim 0.999$, the isolated point-defect regime in which interactions between minority atoms are negligible, (ii) $0.001 \lesssim c \lesssim 0.05$ or $0.95 \lesssim c \lesssim 0.999$, the pair defect regime in which minority atoms are so few that they are unlikely to contribute significantly to the spectra except as isolated atoms or as pairs of atoms, and (iii) $0.05 \lesssim c \lesssim 0.95$, the alloy regime (see Fig. 3).

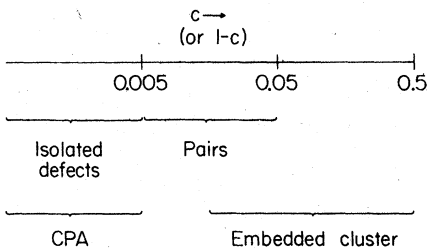

FIG. 3. Schematic diagram of the regions of concentration where various theories are valid and computationally tractable.

A theory of alloys is required only for the last, alloy, regime. Successful theories of isolated and paired defects are well known[7,28,33,34] and one need only evaluate these theories and average the results over all possible alloy configurations. These point- and paired-defect theories are valid for all mass ratios.

For example, in the case of a linear chain with a single isolated impurity, one may solve exactly for the vibrational density of states.[35] For the case of a single light A atom in an otherwise perfect heavy B host, one obtains a change in the density of states from its perfect lattice value of the form[28]

$$\lim_{c\to 0}\frac{d}{dc}D(\omega^2) = -\frac{2\epsilon\omega_B^2}{\pi\omega}\frac{\Theta(\omega)\Theta(2\omega_B-\omega)}{[4\omega_B^2-(1-\epsilon^2)\omega^2](4\omega_B^2-\omega^2)^{1/2}} - \tfrac{1}{2}\delta(\omega^2-4\omega_B^2)+\delta(\omega^2-4\omega_B^2(1-\epsilon^2)^{-1}), \quad (20)$$

where $\epsilon = 1 - m_A/m_B$. Likewise, for an isolated heavy-mass defect B in an otherwise perfect linear chain of light A atoms, the change in the density of states has the form[28]

$$\lim_{c\to 0}\frac{d}{d(1-c)}D(\omega^2) = \frac{2|\epsilon'|\omega_A^2}{\pi\omega}\frac{\Theta(\omega)\Theta(2\omega_A-\omega)}{[4\omega_A^2-(1-\epsilon'^2)\omega^2](4\omega_A^2-\omega^2)^{1/2}} - \tfrac{1}{2}\delta(\omega^2-4\omega_A^2), \quad (21)$$

where $\epsilon' = 1 - m_B/m_A$. These point-mass defect-induced changes in the vibrational densities of states for light and heavy defects are shown in Fig. 4 for the mass ratio $m_B/m_A = 2$.

The effect of a pair of defects on the phonon spectra of a linear-chain host can likewise be evaluated, although a closed-form solution does not exist. By taking an ensemble average over all possible configurations of pairs, one can adequately cover the alloy concentration regime $c \lesssim 0.05$ or $c \gtrsim 0.95$.[34]

The extension of the point- and pair-defect theories to three dimensions is straightforward; the additional computational labor is not prohibitive. Hence, *the theory of alloys need only be concerned with the regime of concentrations for which clusters of three or more minority atoms occupy a significant fraction of configuration space:* $0.05 \lesssim c \lesssim 0.95$.

The most widely used theories of alloy spectra, the virtual crystal approximation, ATA and the CPA, do not reproduce the pair-defect calculations[28,33,34] for $D(\omega^2)$ to order c^2 or $(1-c)^2$ in the concentration and are drastically in error when higher-order cluster effects are important. Therefore, these theories are not generally useful in the alloy regime $0.05 \lesssim c \lesssim 0.95$. (See Fig. 3.) Indeed the virtual crystal model does not correctly give

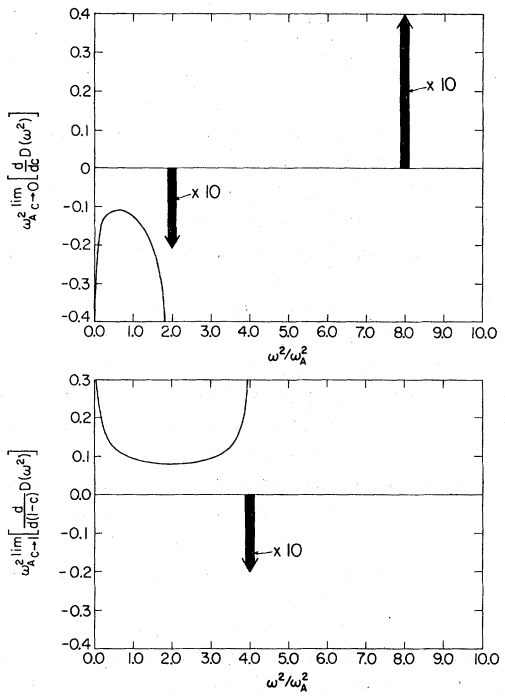

FIG. 4. Change in the one dimensional vibrational density of states for $m_B/m_A = 2$ induced by (a) the presence of an isolated A atom in a pure B host and (b) an isolated B atom in a pure A host. The δ functions in the spectra are represented as boxes whose areas are 1/10 the strength of the δ functions.

the single impurity modifications to $D(\omega^2)$ of order c or $1-c$, while the CPA and ATA fail at orders c^2 and $(1-c)^2$. Hence, in the alloy regime, only two types of theory have proved capable predicting the phonon spectra of one-dimensional binary alloys; the multisite CPA theories[9-27] and the "exact" theories of tens of thousands of atoms[4-6]; both types of theories become almost forbiddingly cumbersome in three dimensions.

B. The persistence-amalgamation coupling constant $(m_B - m_A)\omega^2/\phi$ or mass ratio

In the present linear-chain model, the force constant ϕ is the same for any two nearest-neighbors and ω^2 is of order ϕ/m where m is the lighter mass. Hence the persistence-amalgamation coupling constant is effectively the fractional mass ratio $1 - m_A/m_B$, and we shall discuss the mass ratio $m_B/m_A = \omega_A^2/\omega_B^2$.

For nearly equal masses, the phonon spectra of the perfect A and B crystals will be similar, and so the alloy spectra will be "amalgamations" or hybrids of the A and B spectra.[32] In this amalgamation limit ($m_A \approx m_B$), the virtual crystal approximation forms a satisfactory conceptual framework

but a poor starting point for perturbation theory in powers of the mass difference.[36] Such perturbation theory is an analytic expansion and so cannot converge to the nonanalytic defect perturbed spectrum with, for example, its singular local modes.

For grossly unequal masses, $m_A \gg m_B$ or $m_B \gg m_A$, we have $|(m_B - m_A)\omega^2/\phi| \gg 1$ and a lattice vibration at, say, an A site is incapable of propagating to a B site because of the poor impedance mismatch. That is, the force per unit length ϕ is insufficiently great to overcome the barrier $(m_A - m_B)\omega^2$. In this regime, the light atoms will tend to vibrate in the cages provided by the heavy atoms, and the spectra will tend to divide into two pieces, each of which manifests "persistent" characteristics of its parent atom, either A or B.[32] The low-energy density of states will be dominated by the heavy-atom frequency distribution, whereas the high-energy spectra will exhibit local modes corresponding to "islands" of one, two, or more light atoms in a heavy-atom sea.

A successful theory of lattice vibrations in alloys must produce the above amalgamation- and persistence-type spectra for the appropriate mass ratios.

Of the previously available theories, only the numerically cumbersome "exact[4-6]" and multisite CPA theories[9-27] produce accurate spectra for all amalgamation-persistence coupling constants $(m_B - m_A)\omega^2/\phi$. The CPA itself, although explicitly constructed to reproduce the zero and infinite coupling-constant limits for all concentrations,[32] does not yield accurate spectra for any finite coupling constant: zero coupling constant is not an alloy; infinite coupling constant corresponds to light masses vibrating in massive cages; and the CPA, which does not yield the spectra of defect pairs, cannot simulate the exact theory, which does.

V. EMBEDDED-CLUSTER THEORY

The present theory treats a reference effective medium with the Green's function

$$\underline{g}(\omega) = [\underline{M}_0\omega^2 - \underline{\Phi}_0 - \underline{\Sigma}(\omega) + i0]^{-1} ,$$

where $\underline{M}_0$, $\underline{\Phi}_0$, and $\underline{\Sigma}$ are the mass, force constant and self-energy matrices which characterize the effective medium. Embedded in the effective medium is a cluster of N_c atoms, giving the Green's function for the alloy with this specific configuration of atoms in the cluster:

$$\underline{G}(\omega) = (\underline{M}\omega^2 - \underline{\Phi} + i0)^{-1} . \tag{22}$$

(A general treatment of clusters in effective media has been given by Gonis and Garland,[3] and is similar to the present formalism.) We then define the scattering potential $V^*(\omega)$, which vanishes outside the cluster,

$$\underline{V}^*(\omega) \equiv (\underline{M}_0 - \underline{M})\omega^2 - (\underline{\Phi}_0 - \underline{\Phi} + \underline{\Sigma}) \equiv \underline{V} - \underline{\Sigma} . \tag{23}$$

The alloy Green's function $\underline{G}$ is related to the effective medium Green's function $\underline{g}$ by the Dyson equation

$$\underline{G} = \underline{g} + \underline{g}\underline{V}^*\underline{G} , \tag{24}$$

which need only be solved for atoms within the cluster ($\underline{G} = \underline{g}$ outside). This gives

$$\underline{G} = (\underline{1} - \underline{g}\underline{V}^*)^{-1}\underline{g} . \tag{25}$$

In order to obtain the vibrational density of states, one first calculates the average of $\underline{MG}$ over all ν configurations of N_c-atom cluster,

$$\langle\langle \underline{MG} \rangle\rangle = \nu^{-1} \sum_{\alpha=1}^{\nu} (\underline{MG})_\alpha , \tag{26}$$

where $(\underline{MG})_\alpha$ is the operator for the αth cluster.[37] From $\langle\langle \underline{MG} \rangle\rangle$ one calculates the cluster density of states

$$D(\omega^2; N_c) = -(1/N_c\pi)\,\mathrm{Im}(\mathrm{Tr}_c\langle\langle \underline{MG} \rangle\rangle) \tag{27}$$

and takes this to be an approximation to the alloy state density $D(\omega^2)$. Here Tr_c means a trace over cluster sites only.

One can also calculate the configuration averaged local density of states at the nth atomic site

$$l_n(\omega^2; N_c) = -(1/\pi)\,\mathrm{Im}\langle n|\langle\langle \underline{MG} \rangle\rangle|n\rangle , \tag{28}$$

which should be the same at all sites n if the cluster size is sufficiently large; in practice one selects a central site to minimize the boundary effects. Similarly, a configuration averaged local A or B atomic density of states can be defined in terms of the operator $\underline{S}_{A,n}$ which vanishes unless site n is occupied by an A atom

$$l_n^A(\omega^2; N_c) = -(1/\pi)\,\mathrm{Im}\langle n|\langle\langle \underline{MG}\,\underline{S}_{A,n} \rangle\rangle|n\rangle . \tag{29}$$

Likewise, one can calculate the total density of states of a specific cluster configuration

$$d(\omega^2; N_c) = -(1/N_c\pi)\,\mathrm{Im}[\mathrm{Tr}_c(\underline{MG})] , \tag{30}$$

and the local density of states at the nth atomic site within a given configuration

$$d_n(\omega^2; N_c) = -(1/\pi)\,\mathrm{Im}\langle n|\underline{MG}|n\rangle . \tag{31}$$

Hence, in the embedded cluster method, the procedure for obtaining the vibrational spectrum of the alloy A_cB_{1-c} is: (i) select an alloy composition c as near as possible to the actual composition; this partially specifies the cluster size, because cN_c must be an integer; (ii) enumerate all possible configurations of A and B atoms in a cluster of N_c atoms; (iii) select an effective medium Green's function [here we use the CPA Green's function, Eqs. (9)–(17), because it is self-consistent and in-

dependent of the initial choice of reference lattice, and because it produces better results than the principal alternatives: ATA or virtual crystal (See Appendix)]; (iv) construct the defect matrix $\underline{V}$ for each cluster (for our case of mass disorder only, $\underline{\Phi} = \underline{\Phi}_0$, $\underline{V}$ is diagonal); (v) solve the matrix equation, Eq. (25), for $\underline{G}$; (vi) evaluate the density of states; and (vii) average over all configurations in the cluster.

VI. COMPARISON WITH "EXACT" NUMERICAL RESULTS

A. Density of states

1. Dependence on c for $m_B/m_A = \omega_A^2/\omega_B^2 = 2$

The concentration dependence of the spectra, in comparison with Dean's 8000-atom numerical calculations,[4,5] are displayed in Fig. 5 for a mass ratio of two and for concentrations $c = \frac{1}{6}$, $\frac{1}{3}$, $\frac{2}{3}$, and $\frac{5}{6}$.

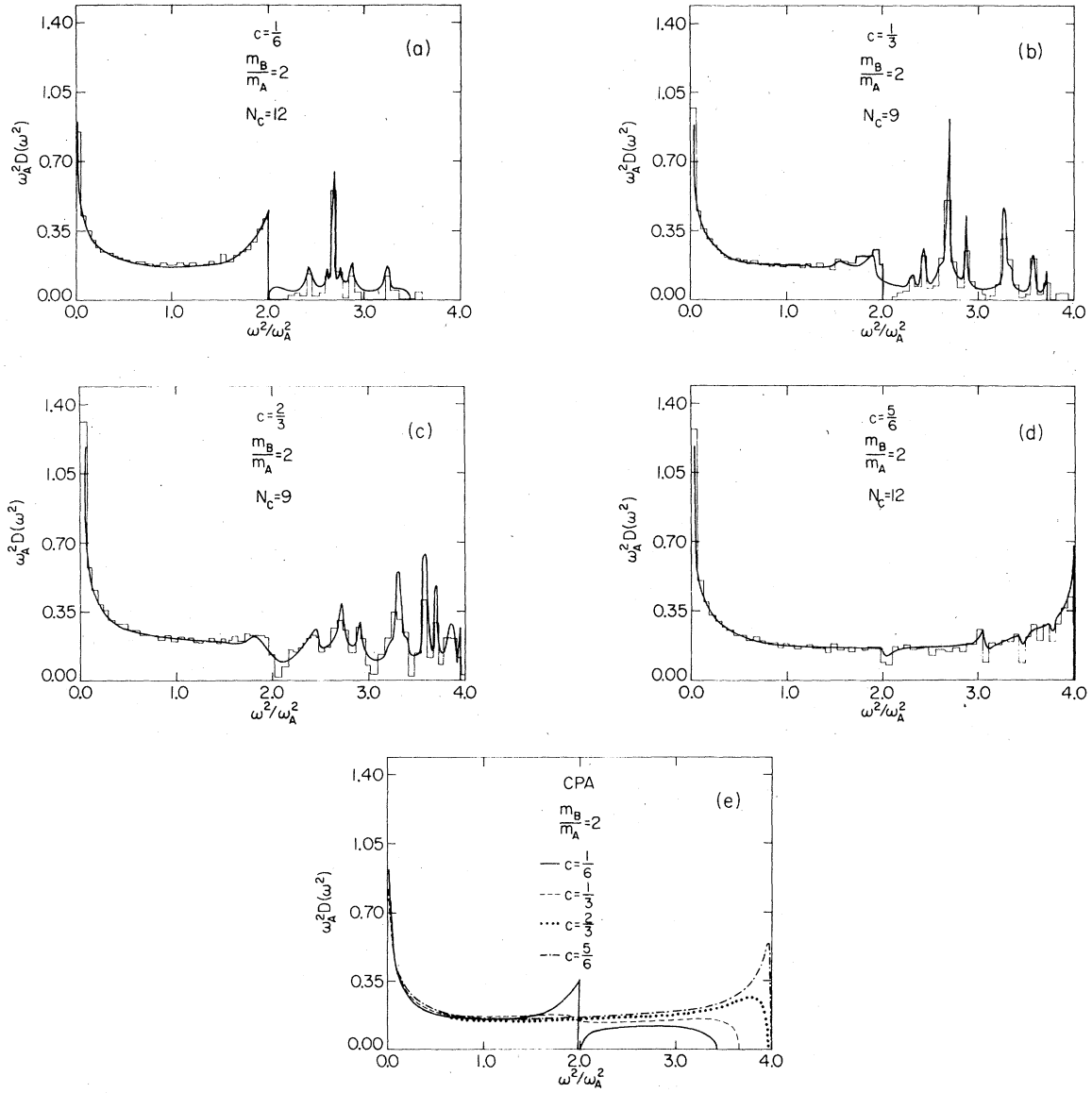

FIG. 5. Vibrational densities of states as functions of c. Histograms are the disordered linear chain A_cB_{1-c} obtained by Dean (Refs. 4, 5) for 8000 atoms. Dark curves are the results obtained by the present embedded cluster method using a cluster of N_c atoms and a CPA effective medium. These are shown for $m_B/m_A = 2$. (a) $c = \frac{1}{6}$, $N_c = 12$, (b) $c = \frac{1}{3}$, $N_c = 9$, (c) $c = \frac{2}{3}$, $N_c = 9$, (d) $c = \frac{5}{6}$, $N_c = 12$; (e) the coherent-potential approximation shown as a function of c, Dean's results are for $c = 0.16$, 0.38, 0.62, and 0.84, respectively.

Corresponding results for $c=\frac{1}{2}$ and mass ratio 2 are compared with 100 000-atom calculation of Payton and Visscher[6] in Fig. 1(c). Our calculations for $c=\frac{1}{6}$ and $\frac{5}{6}$ were performed on 12-atom clusters; those for $c=\frac{1}{3}$ and $\frac{2}{3}$ were obtained for nine atom clusters; and, for the $c=\frac{1}{2}$ results, a ten-atom cluster was used. The calculations produce all the principle features of the "exact" spectra. The sole unsatisfactory feature is the fact that the theory produces no states at frequencies where the CPA has no states. For reference the CPA results are displayed in Fig. 5(e).

It is roughly as easily computationally to evaluate the spectra for $c=\frac{1}{6}$ and a 12-atom cluster as for $c=\frac{1}{3}$ and a 9-atom cluster. Also the Dean calculations displayed here are for small 8000-atom chains, and not all of the discrepancy between the present theory and Dean's results are ascribable to the present work.

2. Dependence on $\omega_A^2/\omega_B^2 = m_B/m_A$ for $c = 1/2$

The frequency spectra change dramatically as the mass ratio is varied (5:4, 3:2, 10:1), as illustrated in Fig. 6 in comparison with Payton and Visscher's 8000-atom calculations. Figure 1(c) gives comparable results for a 2:1 mass ratio in comparison with a 100 000-atom calculation by Payton and Visscher. The CPA results are included in Fig. 6(d) for reference. Observe that the clusters all contain ten atoms, and that the theory is in excellent agreement with the "exact" results.

3. Dependence on cluster size: $c = 1/2$, $m_B/m_A = \omega_A^2/\omega_B^2$

Calculations for cluster sizes of $N_c=2$, 4, 6, 8, and 10 are given in Fig. 7, and illustrate how the various peaks originate from the various-size clusters; the embedded cluster theory simulates the "exact" spectrum quite well for $N_c=6$ and moderately well for $N_c=4$.

B. Local densities of states

The local densities of states are as easily computed as the total densities of states. Configuration-averaged local state densities at A and B sites are displayed in Fig. 8.

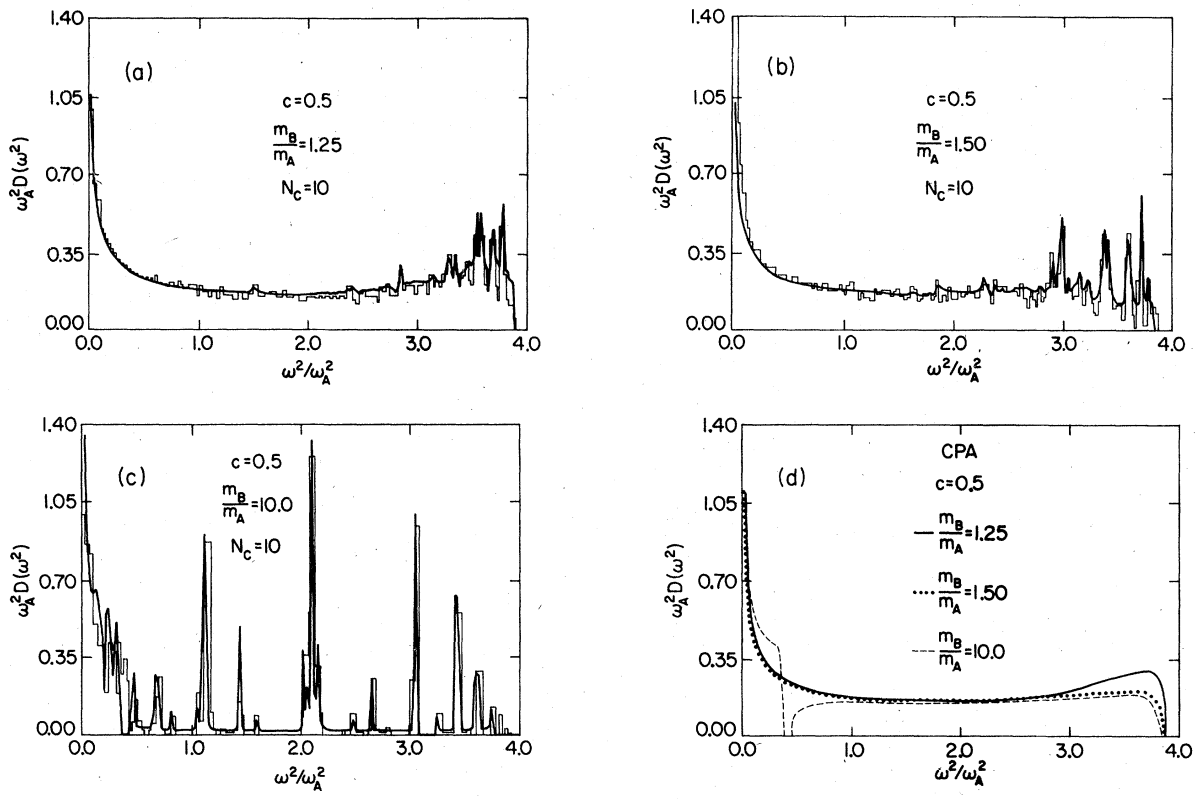

FIG. 6. Vibrational state densities as function of m_B/m_A. Histograms are the exact vibrational densities of states for the disordered linear chain A_cB_{1-c} obtained by Payton and Visscher (Ref. 6) for 8000 atoms. Dark curves are the results obtained by the present embedded cluster method using a cluster of 10 atoms and a coherent-potential approximation (CPA) effective medium. These are shown for $c=0.5$. (a) $m_B/m_A=1.25$, (b) $m_B/m_A=1.50$, (c) $m_B/m_A=10.0$, (d) CPA for $m_B/m_A=1.25$, 1.50, and 10.0.

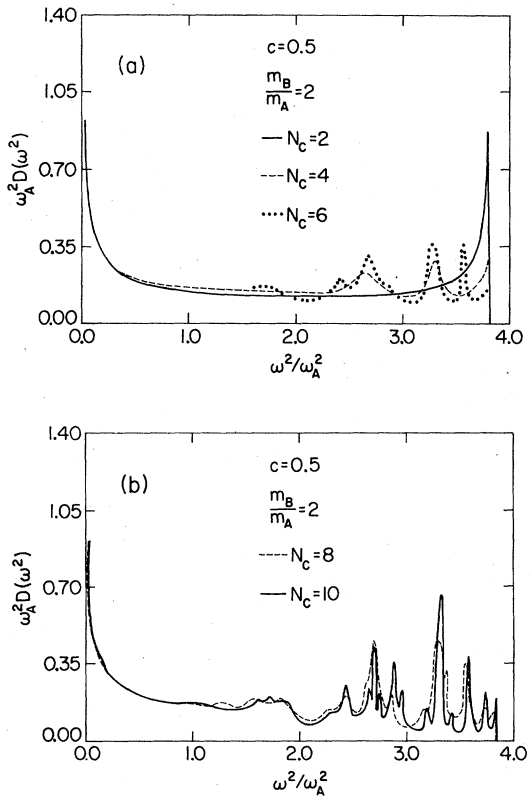

FIG. 7. Dependence on cluster size N_c: Embedded cluster method results for the vibrational density of states for the disordered chain A_cB_{1-c} for the case $c=0.5$, $m_B/m_A=2$, for (a) $N_c=2,4,6$, and (b) $N_c=8$ and 10.

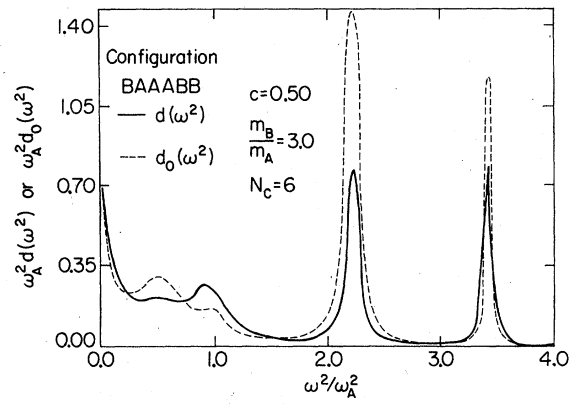

FIG. 9. Total and local central-site densities of states $d(\omega^2)$ and $d_0(\omega^2)$ for the cluster configuration *BAAABB* and $c=0.5$, $m_B/m_A=3$.

C. Single configurations and nonrandom alloys

The local and global densities of states for any single configuration within the cluster can be easily calculated. Figure 9 shows the results for a typical cluster: three light atoms surrounded by heavy ones.

Such individual cluster calculations permit one to identify spectral signatures characteristic of specific atomic configurations, and therefore should facilitate analyses of nonrandom alloys. To illustrate this point, Fig. 10 gives a total and local central site random-alloy spectra for the same case as shown in Figs. 8 and 9, but labels the peaks associated with one, two, and three light atoms vibrating within heavy atom cages. If the alloy were not random and if A atoms tended to

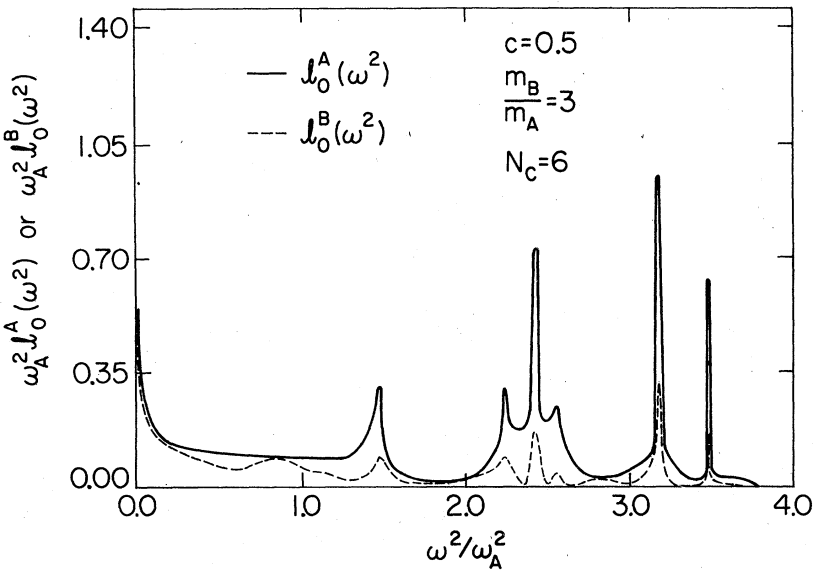

FIG. 8. Configuration-averaged local densities of states $J_0^A(\omega^2)$ and $J_0^B(\omega^2)$ at sites A and B, respectively, for $c=0.5$, $m_B/m_A=3$, $N_c=6$.

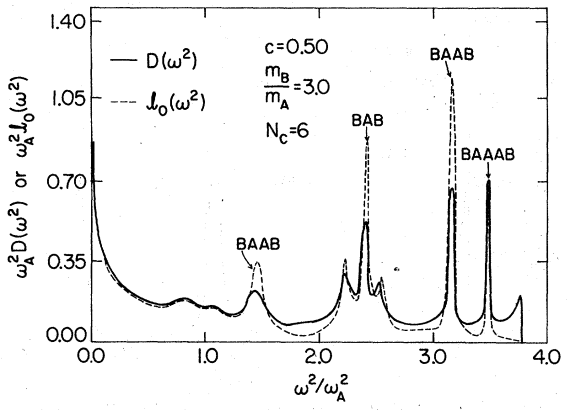

FIG. 10. Total and local configuration-averaged densities of states for $N_c=6$, $c=0.5$, and $m_B/m_A=3$. Peaks associated with specific atomic clusters are labeled.

cluster, then the *BAB* and *BAAB* lines would be weaker and the *BAAAB* line would be stronger. Hence alloy measurements which are sensitive probes of the state density can be used in conjunction with such calculations to determine the existence and nature of clustering and nonrandom disorder.

VII. DISCUSSION

The present embedded cluster method successfully reproduces the "exact" numerical vibrational densities of states in one dimension for all concentrations and all mass ratios (or persistence-amalgamation coupling constants). It does so with a small cluster size, and still satisfies the oscillator strength sum rule. The theory produces the correct spectra in the exactly soluble limits $c \to 0$ and $c \to 1$. The greatest assets of the theory are that it converges for small cluster size, that it can be generalized to apply to ternary[2] and quaternary alloys, that it appears eminently applicable to calculations of vibrational spectra in real three dimensional alloys, and that it is particularly well adapted to the alloy regime $0.05 \lesssim c \lesssim 0.95$ which is inaccessible to virtually all of the widely-used theories of alloys.

A feature of the present theory is that it permits identification of various peaks in the density of states with specific alloy configurations. Therefore, one can imagine employing the theory to study nonrandom alloys in which atoms of one species cluster together. For example, if measurements should prove inconsistent with a random alloy theory, one could determine the types of nonrandom alloying consistent with the observations by using this theory.

The embedded cluster theory, when combined with pair-defect calculations for low alloy concentrations ($c \lesssim 0.05$), provides the most efficient way to compute alloy spectra.

A comparison of the numerical efficiency of the various theoretical schemes illustrates the advantages of the present method. A numerical calculation such as that of Dean[4,5] or Payton and Visscher[6] for a three-dimensional cube with as many atoms on an edge as contained in their one-dimensional chains would require manipulation of matrices of size $(3\times10^{15})\times(3\times10^{15})$ instead of $10^5 \times 10^5$ in one dimension. Even with the unrealistic simplifying assumption that the disorder is diagonal (solely mass disorder), the numerical problem is feasible only for very small atomic clusters $(10\times10\times10)$.

Extensions of the CPA to self-consistent multisite approximations offer comparable computational obstacles[9-27]: for a $10\times10\times10$ atom-cluster self-consistent solution, one must manipulate $(3\times10^3)\times(3\times10^3)$ matrices which depend on four variables, wave vector $\vec{k}$ and frequency ω. These matrix equations must be iterated to convergence for every $\vec{k}$ and ω. By contrast, the embedded cluster theory does not iterate the cluster to self-consistency and the reference medium self-energy is independent of $\vec{k}$ (in one dimension it can be evaluated easily by solving a cubic equation). The resulting calculation is simpler than multisite CPA by a factor $\sim N_c^2 I \sim 10^7$, where I is the number of iterations required for self-consistency.

The principal drawbacks of the method are not serious: (i) the $c \to 0$ and $c \to 1$ regimes are more easily treated by performing single- and paired-defect calculations; (ii) the concentration must be a rational number, cN_c = integer; and (iii) the effective medium Green's function, as presently obtained using the CPA, is not fully satisfactory, it causes the local-mode bandwidth to be too narrow [Figs. 1(c), 5, 6,].

Future work should examine the possibility of obtaining a more easily calculated effective-medium Green's function, which describes more satisfactorily the high-frequency limits of the spectra. The present work, however, does seem to be leading us to the point where realistic alloy calculations will be feasible in three dimensions as well as in one.

Finally, we note that the methods presented here can be easily applied to electronic and magnetic excitations of alloys, as well as to vibrational spectra.

ACKNOWLEDGMENTS

This work was supported by the U. S. Office of Naval Research under Contract No. N00014-77-C-0537. The authors thank P. Vogl, C. P. Flynn,

H. Kaga, and D. Stroud for constructive suggestions.

APPENDIX: USE OF THE AVERAGE-T-MATRIX EFFECTIVE MEDIUM WITH THE EMBEDDED-CLUSTER METHOD

The calculations presented in the text were performed using a cluster embedded in the CPA effective medium. In general, however, the calculations outlined in Eqs. (22)–(25) could be performed using any effective medium. One obvious medium is that given by the average-T-matrix approximation (ATA).[7] The ATA has the potential advantage that, since it is not a self-consistent approximation it is easier to compute than the CPA; this is particularly true for the case of real three dimensional alloys. We have therefore tested our method using the ATA effective medium at the cluster boundary.

Since the ATA is a non-self-consistent theory, its precise form depends on the choice of reference lattice. It has been found[38] that the best ATA is obtained using the virtual crystal Green's function

$$\underline{G}^{v}(\omega) = \langle\langle \underline{M} \rangle\rangle \omega^2 - \underline{\Phi} + i0)^{-1} , \tag{A1}$$

where we have

$$\langle n | \langle\langle \underline{M} \rangle\rangle | n \rangle = m^* = c m_A + (1-c) m_B . \tag{A2}$$

The ATA self-energy then becomes[38]

$$\underline{\Sigma}_A = \sum_n |n\rangle \sigma_A(\omega) \langle n| , \tag{A3}$$

where

$$\sigma_A(\omega) = \frac{(m^*/m_B)(m_B - m_A)^2 c(1-c)\omega^4 \langle n | G^v(\omega^2) | n \rangle}{1 - (1-2c)(m_B - m_A)\omega^2 \langle n | G^v(\omega^2) | n \rangle} . \tag{A4}$$

By the use of Eqs. (A3) and (A4), one can obtain the ATA effective medium Green's function,

$$\underline{g}^{A}(\omega) = [\langle\langle \underline{M} \rangle\rangle \omega^2 - \underline{\Phi} - \underline{\Sigma}_A(\omega) + i0]^{-1} . \tag{A5}$$

Once $g^A(\omega)$ is known, one may proceed with the steps outlined in Eqs. (22)–(27) to obtain the alloy density of states in the embedded-cluster method. We have done this for several values of the concentration c and for several values of the mass ratio m_B/m_A. Typical results are shown in Fig. 11(a) which illustrates the case $c = 0.25$ and $m_B/m_A = 3$ with a cluster size $N_c = 8$. Also shown in that figure are the exact results obtained by Dean[4,5] for an 8000-atom linear chain. As may be seen from the figure, although some of the peaks in the exact spectrum are approximately reproduced by this calculation, a large, almost structureless, bump is predicted in a region of the spectrum where the exact calculation shows no peaking.

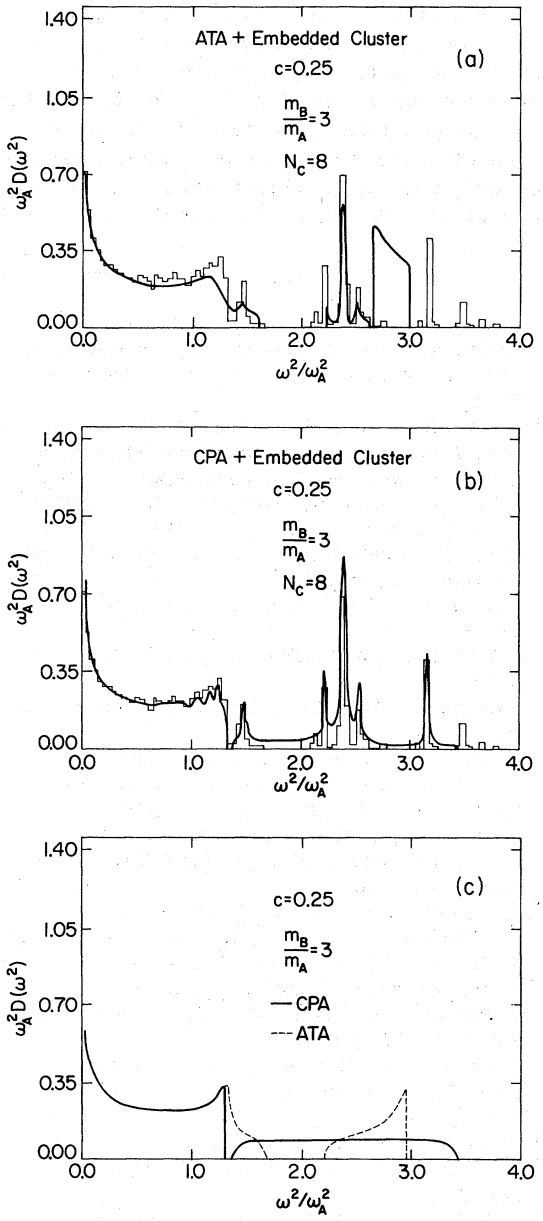

FIG. 11. Comparison of ATA, CPA, and Dean's numerical calculations for $c = 0.25$ and $m_B/m_A = 3$. The dark lines in (a) and (b) correspond to $N_c = 8$ atom clusters embedded in ATA and CPA effective media, respectively. Dean's calculations are for $c = 0.26$. The ATA and CPA without clusters are shown in (c).

By contrast, Fig. 11(b) illustrates the results obtained for this case using the embedded cluster method with $N_c = 8$ and a CPA effective medium. Clearly, the cluster embedded in the CPA medium gives the better results, yielding a spectrum which reproduces all of the major features of the exact spectrum.

It is thus clear that the embedded cluster method, when used with an ATA effective medium, fails to adequately reproduce the exact results for the same cluster size for which the use of a CPA medium yields excellent results. Physically, this means that the CPA effective medium more accurately mimics the vibrational response of the true alloy at the cluster surface than does the ATA. This is an illustration of the fact that the CPA is the best single-site effective medium possible.[7] Some of the difficulties with the ATA medium could conceivably by partially diminished by using very much larger cluster sizes, but then the virtues of a simpler effective medium would be offset by the necessity to carry out matrix manipulation with very large matrices.

---

*Present address: Dept. of Physics and Engineering Physics, Texas Tech. University, Lubbock, Texas 79409.

[1]D. J. Wolford, B. G. Streetman, W. Y. Hsu, and J. D. Dow, *Proceedings of the Thirteenth International Conference on the Physics of Semiconductors, Rome, 1976*, edited by F. G. Fumi, (Tipografia Marves, Rome, 1976), p. 1049; W. Y. Hsu, J. D. Dow, D. J. Wolford, and B. G. Streetman, Phys. Rev. B 16, 1597 (1977) and references therein.

[2]C. W. Myles and J. D. Dow, Phys. Rev. Lett. 42, 254 (1979).

[3]A. Gonis and J. W. Garland, Phys. Rev. B 16, 2424 (1977).

[4]P. Dean, Rev. Mod. Phys. 44, 127 (1972) and references therein.

[5]P. Dean, Proc. R. Soc. A 260, 263 (1961).

[6]D. N. Payton and W. M. Visscher, Phys. Rev. 154, 802 (1967); 156, 1032 (1967); 175, 1201 (1968).

[7]See for example, R. J. Elliott, J. A. Krumhansl, and P. L. Leath, Rev. Mod. Phys. 46, 465 (1974) and references therein.

[8]I. M. Lifshitz, Adv. Phys. 13, 483 (1964).

[9]R. L. Jacobs, J. Phys. F 3, 933 (1974); 4, 1351 (1974).

[10]N. Zaman and R. L. Jacobs, J. Phys. F 5, 1677 (1975).

[11]K. Aoi, Solid State Commun. 14, 929 (1974).

[12]F. Brouers, M. Cyrot, and F. Cyrot-Lackmann, Phys. Rev. B 7, 4370 (1973).

[13]F. Brouers, F. Ducastelle, and J. Van der Rest, J. Phys. F 3, 1704 (1973).

[14]F. Brouers and F. Ducastelle, J. Phys. F 5, 45 (1975).

[15]T. Miwa, Prog. Theor. Phys. 52, 1 (1974).

[16]N. F. Berk and R. A. Tahir-Kheli, Phys. Rev. B 8, 2496 (1973).

[17]A. R. Bishop and A. Mookerjee, J. Phys. C 7, 2165 (1973).

[18]P. Lloyd and P. R. Best, J. Phys. C 8, 3752 (1975); P. R. Best and P. Lloyd, J. Phys. C 8, 2219 (1975).

[19]M. Tsukada, J. Phys. Soc. Jpn. 32, 1475 (1972).

[20]I. Takahashi and M. Shimizu, Prog. Theor. Phys. 51, 1678 (1973).

[21]S. Wu, J. Math. Phys. 15, 947 (1974).

[22]S. Wu and M. Chao, Phys. Status Solidi B 68, 349 (1975).

[23]C. T. White and E. N. Economou, Phys. Rev. B 15, 3742 (1977).

[24]W. H Butler, Phys. Rev. B 8, 4499 (1973).

[25]F. Ducastelle, J. Phys. C 7, 1795 (1975); J. Phys. F 2, 468 (1972).

[26]W. H. Butler and B. G. Nickel, Phys. Rev. Lett. 30, 373 (1973).

[27]V. Capek, Phys. Status Solidi B 43, 61 (1971); Czech. J. Phys. B 21, 997 (1971); Phys. Status Solidi B 52, 399 (1972).

[28]See, for example, A. A. Maradudin, E. W. Montroll, G. H. Weiss, and I. P. Ipatova, in *Solid State Physics, Supplement 3*, 2nd ed., edited by H. Ehrenreich, F. Seitz, and D. Turnbull (Academic, New York, 1971), Chap. III.

[29]P. Soven, Phys. Rev. 156, 809 (1967).

[30]D. W. Taylor, Phys. Rev. 156, 1017 (1967).

[31]B. Velicky, S. Kirkpatrick, and H. Ehrenreich, Phys. Rev. 175, 747 (1968).

[32]Y. Onodera and Y. Toyozawa, J. Phys. Soc. Jpn. 24, 341 (1968).

[33]See, for example, the exhaustive review by A. A. Maradudin, in *Solid State Physics, 1966*, edited by F. Seitz and D. Turnbull (Academic, New York, 1966), Vols. 18–19.

[34]E. W. Montroll and R. B. Potts, Phys. Rev. 102, 72 (1956).

[35]One uses the formalism

$$\underline{G} = \underline{G}^0 + \underline{G}^0 \underline{V} \underline{G} ,$$

where

$$\underline{V} = (\underline{M}_0 - \underline{M})\omega^2 = \underline{V}_0 \mid 0\rangle \langle 0 \mid .$$

[36]See, for example, J. Pirenne, Physica 24, 73 (1958).

[37]In general there are $\nu = \binom{N_c}{l}$ configurations for a cluster of N_c atoms and a composition $c = l/N_c$. Of course, not all ν configurations are physically distinct.

[38]P. L. Leath and B. Goodman, Phys. Rev. 181, 1062 (1969).